THERAPEUTIC APHERESIS

Review

Recent advances in microfluidic cell separation to enable centrifugation-free, low extracorporeal volume leukapheresis in pediatric patients

Mubasher Iqbal[1], Anton Mukhamedshin[1], Dalia L. Lezzar[1], Kumar Abhishek[1], Alexandra L. McLennan[2], Fong W. Lam[2], Sergey S. Shevkoplyas[1]

[1]*Department of Biomedical Engineering, University of Houston, Houston, TX, United States of America;* [2]*Division of Pediatric Critical Care Medicine, Baylor College of Medicine, Houston, TX, United States of America*

Leukapheresis is a common extracorporeal procedure for leukodepletion and cellular collection. During the procedure, a patient's blood is passed through an apheresis machine to separate white blood cells (WBCs) from red blood cells (RBCs) and platelets (PLTs), which are then returned to the patient. Although it is well-tolerated by adults and older children, leukapheresis poses a significant risk to neonates and low-weight infants because the extracorporeal volume (ECV) of a typical leukapheresis circuit represents a particularly large fraction of their total blood volume. The reliance of existing apheresis technology on centrifugation for separating blood cells limits the degree to which the circuit ECV could be miniaturized. The rapidly advancing field of microfluidic cell separation holds excellent promise for devices with competitive separation performance and void volumes that are orders of magnitude smaller than their centrifugation-based counterparts. This review discusses recent advancements in the field, focusing on passive separation methods that could potentially be adapted to perform leukapheresis. We first outline the performance requirements that any separation method must meet to replace centrifugation-based methods successfully. We then provide an overview of the passive separation methods that can remove WBCs from whole blood, focusing on the technological advancements made in the last decade. We describe and compare standard performance metrics, including blood dilution requirements, WBC separation efficiency, RBC and PLT loss, and processing throughput, and discuss the potential of each separation method for future use as a high-throughput microfluidic leukapheresis platform. Finally, we outline the primary common challenges that must still be overcome for these novel microfluidic technologies to enable centrifugation-free, low-ECV leukapheresis in the pediatric setting.

Keywords: *leukapheresis, microfluidics, cell separation, pediatrics.*

© SIMTIPRO Srl

INTRODUCTION

Leukapheresis is a complex medical procedure during which blood is continuously removed from a patient by an apheresis machine to separate leukocytes (white blood cells, WBCs) from the rest of the blood, which is then returned to the patient[1]. This procedure is used for two main applications in medicine: leukodepletion (to urgently

Arrived: 10 November 2022
Revision accepted: 2 March 2023
Correspondence: Sergey S. Shevkoplyas
e-mail: sshevkoplyas@uh.edu

© SIMTIPRO Srl

reduce a dangerously elevated WBC count) and cellular collection (to harvest various WBC subsets for manufacturing cellular therapies)[2,3].

Leukodepletion is indicated in patients exhibiting symptomatic hyperleukocytosis, which is defined as a circulating WBC count of >100,000/μL and can occur in patients with acute lymphoblastic or acute myeloid leukemia (ALL and AML, respectively). The lymphoblasts (ALL) and myeloblasts (AML) seen in leukemia may lead to leukostasis due to the increased blood viscosity and decreased deformability of the abnormal cells[4,5]. Additionally, there may be increased adhesion of leukemic cells to vascular endothelium, potentially due to increased expression of cellular adhesion molecules on endothelial cells induced by cytokines released by blasts[6]. Leukostasis in the microcirculation causes tissue hypoxia/ischemia and organ dysfunction which, when occurring in the brain and lungs, results in severe complications such as stroke, acute lung injury, and pulmonary hypertension[7]. In addition to leukostasis, hyperleukocytosis predisposes leukemic patients to the risks of blast lysis and dangerous electrolyte/chemical derangement, known as tumor lysis syndrome[8]. Mortality in patients with acute leukemia presenting with hyperleukocytosis can be as high as 40% within the first month, and lower WBC count is associated with fewer early deaths[9,10]. Leukapheresis is used to rapidly remove excessive WBCs and thus alleviate hyperleukocytosis symptoms in ALL and AML while cytoreductive chemotherapy is taking effect[10–14]. The American Society of Apheresis has listed leukapheresis as a category II indication ("Disorders for which apheresis is accepted as second-line therapy, either as a standalone treatment or in conjunction with other modes of treatment") for symptomatic hyperleukocytosis and category III ("Optimum role of apheresis therapy is not established. Decision making should be individualized") for asymptomatic hyperleukocytosis in patients with ALL or AML[15]. In addition, the ability to rapidly reduce the number of activated WBCs in a patient's blood has made leukodepletion an attractive drug-free treatment for several emergent indications, including inflammatory bowel disease[16–18], steroid-resistant nephrotic syndrome[19], critical pertussis in infants[20,21], and refractory systemic juvenile idiopathic arthritis[22].

Cellular collection via leukapheresis is the key initial step for an increasing number of highly effective cell-based treatments for some of the most devastating disorders affecting millions of adults and children worldwide[3]. For instance, CD34+ cells obtained via leukapheresis have become a common source of grafts for hematopoietic stem cell transplantation[23–25] and the initial cellular material for novel gene-based therapies designed to cure sickle cell disease and β-thalassemia[26,27]. CD14+ monocytes isolated from leukapheresis samples are used for generating patient-derived, tumor antigen-loaded dendritic cells to treat various malignancies, including medulloblastoma[28]. CD3+ lymphocytes (T cells) are used to manufacture a rapidly expanding number of chimeric antigen receptor (CAR) T cell therapies for treating hematologic malignancies and other types of cancer[29,30]. CD56+ lymphocytes (NK cells) are engineered to attack tumors that may evade T cell recognition[31]. Less frequently, granulocytes are collected by leukapheresis for transfusion to high-risk neutropenic patients with known bacterial or fungal infections that are unresponsive to regular antimicrobial therapies[32,33].

Depending on the case, the required cells may be collected from the patient themselves (autologous) or from a healthy volunteer donor (allogeneic)[3]. Allogeneic leukapheresis represents a fairly small fraction of all apheresis procedures conducted on healthy individuals, and it is usually performed separately from the significantly more common apheresis collections of platelets (PLTs) and red blood cells (RBCs)[34,35]. However, the frequency of allogeneic leukapheresis varies greatly depending on the required cell type and specific therapy: for example, granulocyte donations are almost always allogeneic, while lymphocyte collections for CAR T cell therapies are generally autologous[3].

Currently, leukapheresis for both therapeutic leukodepletion and cellular collection is performed using centrifugation-based apheresis machines, which separate WBCs from RBCs and PLTs based on the differences in the mass density of the cells[1,3]. Leukapheresis is generally well-tolerated by most adults and older children (minor side effects include nausea, headaches, and musculoskeletal pain). However, performing this procedure in neonates and low-weight

© SIMTIREC Srl

infants is much more technically challenging and clinically risky[1,36-40]. Centrifugation-based apheresis machines have a substantial extracorporeal volume (ECV), typically ranging from 150 to 250 mL[3], while the total blood volume (TBV) of a 4 kg neonate is only ~400 mL, and ~800 mL for a 10 kg infant[36,37,41,42]. Because ECV represents a particularly large fraction of their TBV, these vulnerable patients experience a significantly higher incidence of hypotension, symptomatic hypocalcemia, allergic reactions, catheter-related thrombosis, infections, severe anemia, and even death[36,38-40]. The use of centrifugation by conventional apheresis machines limits the degree to which their ECV could be minimized. Therefore, new approaches to cell separation are urgently needed to enable low-ECV leukapheresis, particularly in pediatric patients.

Microfluidic cell separation could offer an exciting and safer alternative to centrifugation-based apheresis because of the high separation efficiency and innately small void volumes microfluidic devices could have. Passive separation methods are particularly attractive because devices based on these methods are generally simpler to fabricate and operate and can be easily adapted to work with existing supporting technologies such as medical-grade tubing, pumps, and other extracorporeal devices. This review aims to discuss recent advancements in microfluidic cell separation with a focus on passive methods that could potentially be adapted to perform leukapheresis. We first outline the performance requirements that any separation technology must meet to be competitive with centrifugation-based methods. We then provide an overview of the passive separation methods that can separate WBCs from whole blood (WB), focusing on the technological advancements made in the last decade. We describe and compare standard performance metrics, including blood dilution requirements, WBC separation efficiency, RBC and PLT loss, and processing throughput, and discuss the potential of each separation method as a future microfluidic leukapheresis platform. Finally, we outline the remaining challenges that must still be overcome for these novel microfluidic technologies to enable centrifugation-free, low-ECV leukapheresis in pediatric patients.

OPERATING PARAMETERS AND SEPARATION PERFORMANCE IN CURRENT LEUKAPHERESIS PRACTICE

Centrifugation-based leukapheresis for leukodepletion

A typical pediatric patient undergoing leukodepletion is severely anemic with hemoglobin (Hb) of ~7 g/dL, or ~20-25% hematocrit (HCT), and has a WBC count far exceeding the 100×10^3/μL threshold ($300\text{-}500\times10^3$/μL on average, and can be as high as 900×10^3/μL)[43,44]. Before the procedure, the extracorporeal circuit is primed with saline and the anticoagulant citrate dextrose solution formula A (ACD-A) or with a unit of packed RBCs (if the ECV exceeds the patient's TBV by more than ~10%). During the procedure, the patient's blood is processed at a flow rate of 10-25 mL/min, with the anticoagulant added continuously at the ACD-A:blood ratio of 1:12-15 and the WBC fraction collected at the rate of 3-7 mL/min. For instance, Zeng *et al.* reported that the volume of processed blood was 1,888±612 mL, using 136±45 mL of ACD-A for anticoagulation, while collecting 285±97 mL of the WBC fraction[43]. A single leukapheresis procedure may reduce the WBC count by ~35% when processing 1-2 TBV and by ~50% when processing 2-3 TBV, although the effectiveness of leukoreduction varies widely between patients. In fact, the stated objective of reducing the WBC count below 100×10^3/μL is rarely accomplished in just one procedure[43,44]. Because centrifugation of WB typically creates a clear separation between the RBC and buffy coat layers, the RBC losses are relatively low; therefore, patients' HCT remain virtually unchanged by the procedure[43]. However, the buffy coat layer contains a significant fraction of PLTs, which are removed at similar rates as WBCs. In the same study, Zeng *et al.* reported that the reduction of PLTs (31±14%) was similar to that of WBCs (35±15%) after a single leukodepletion procedure[43]. The drop in PLT counts could exacerbate bleeding from catheter sites or, worse, lead to hemorrhagic conversion of strokes due to cerebral leukostasis[45].

Centrifugation-based leukapheresis for cellular collection

A typical pediatric patient undergoing leukapheresis for cellular collection is moderately anemic (Hb of ~9-10 g/dL, or ~30% HCT) and has a WBC count ranging from as low as 0.5×10^3/μL to as high as 85×10^3/μL[30,46-48]. The leukapheresis

© SIMTIRO Srl

Blood Transfus 2023; 21: 494-513 doi: 10.2450/BloodTransfus.506

circuit is primed with irradiated, leukocyte-depleted packed RBCs for patients weighing less than 20-30 kg, those with severe anemia, or for whom ECV is greater than ~10% of their TBV[30,46-48]. Because the cells of interest can be scarce (pre-apheresis counts of <100/μL for CD34+ cells[47] and <150/μL for CD3+ cells[30]), leukapheresis collections are often performed by processing 3-5 TBV[46,48]. To process such a large volume of blood in a reasonable amount of time (<300 min[46,48]), inlet flow rates ranging from 10-50 mL/min[47,48], and in some cases even as high as 100 mL/min[30], are used. Because the inlet flow rate is limited by how much ACD-A can be infused safely, heparin is added to provide anticoagulation while reducing the ACD-A:blood ratio to less than 1:20, thus mitigating the risk of citrate toxicity and circulatory overload at high flow rates[30,46]. The separated WBC fraction is collected at a rate of ~1 mL/min to minimize the patient's blood volume loss[30,46-48]. For example, in one study of CD34+ cell collection, the median volume of processed WB was 4957 mL (range 2,101-8,672 mL), and the median volume of infused ACD-A was 240 mL (range: 113-416 mL); the blood was processed at a median inlet flow rate of 22 mL/min (range: 10-47 mL/min), and separated WBC fraction was collected at a rate of 1.0 mL/min for a total volume of 242 mL (range: 191-304 mL)[46]. While the loss of RBCs is typically low, the depletion of PLTs when performing large-volume leukapheresis may be significant[46,47]. At the same time, a high level of contamination of the collected WBC fraction by RBCs and PLTs may interfere with downstream cellular therapy manufacturing steps[49]. In the study of CD34+ cell collection referenced above, the leukapheresis procedure reduced the median WBC count by 37% and the median PLT count by 49%, while Hb was reduced by only 12%[46].

Design goals for future microfluidics-based leukapheresis

In addition to separating WBCs from RBCs and PLTs with high efficiency, any future microfluidics-based leukapheresis platform will need to demonstrate the following functionality to meet or exceed the performance expectations outlined above:

- Operate in a recirculation regime to return RBCs, PLTs, and plasma to the patient.
- Reduce ECV to <10% of a patient's TBV to avoid priming the circuit with stored RBCs and minimize the effect of the procedure on the patient's hemodynamics.
- Work for whole blood with HCT in the range of 20-40% and WBC count as high as 300×10^3/μL.
- Minimize the loss of RBCs and PLTs (<10%) to reduce the need for blood transfusion after the procedure.
- Be compatible with ACD-A, heparin, and (potentially) other anticoagulants approved by the FDA for use in human subjects undergoing leukapheresis.
- Achieve the inlet flow rate of at least 10 mL/min for the procedure duration to be comparable to conventional leukapheresis.
- Process large volumes (liters) of whole blood without clogging or a decline in separation efficiency.
- Prevent damage to the cells to mitigate adverse outcomes after the procedure and preserve the viability and functional properties of collected WBCs.

MICROFLUIDIC TECHNOLOGIES FOR SEPARATING WBCS FROM WHOLE BLOOD

In their work on the continuous flow microfluidic diffusive filter, Sethu *et al.* were the first to propose using microfluidic devices for performing leukapheresis[50]. Since then, the field of microfluidic cell separation has undergone significant development, with several technologies showing great potential to finally accomplish that goal. The microfluidic techniques for separating WBCs from whole blood can be categorized broadly into active and passive methods. Active methods rely on external forces such as the magnetic, acoustophoretic, or dielectrophoretic force (or their combination) to separate the target cells and direct them into specific outlets. These methods generally allow for excellent control over the positions of the cells of interest within the device, leading to high-purity separations[46,51]. However, these methods typically require extensive sample preparation (such as RBC lysis) and complex setups, making them impractical for many clinical settings[51-54]. In contrast, passive separation methods exploit properties intrinsic to the device or the sample, such as the channel geometry and the hydrodynamic forces occurring due to the flow of the sample in the device, as well as the differences in cell shape, size, and deformability[54,55]. This review focuses on the passive separation methods because they are generally simpler to fabricate, do not require a power source or complex control systems to operate, can process whole blood directly with minimal sample preparation,

© SIMTIPRO Srl

and are easier to interface with downstream sample processing, making passive cell separation methods a particularly attractive choice for replacing conventional centrifugation[54,56,57].

Table I compares the different categories of passive microfluidic cell separation technologies in terms of their characteristics relevant in the context of leukapheresis. When describing individual devices, the separation performance is reported using a set of common metrics either as given by the authors or calculated using the available data to simplify comparisons. For example, in this review, "*WBC recovery*" was defined as the percentage of WBCs of the input sample collected in the WBC-rich output sample, "*WBC purity*" as the percentage of cells in the output sample that are WBCs, and "*RBC loss*" as the percentage of RBCs in the input sample that were not collected in the WBC-rich outlet sample. While most reviewed papers adhered to these definitions, some defined the metrics of separation performance differently or had their own terminology altogether. In such cases, both the original metrics and the recalculated values of the standard metrics were provided.

Filtration through porous membranes and micropillar arrays

Microfluidic separation methods that utilize filtration to separate WBCs from other blood cells by size typically fall into one of two broad categories: dead-end filtration (or microfluidic trapping) and crossflow filtration. In devices that implement dead-end filtration, blood is pushed through a porous membrane, and WBCs (which are larger than the pores) are retained on the surface of the membrane (**Figure 1a**). Microfluidic trapping, a generalization of dead-end filtration, utilizes transient plugging of a microfabricated filter element (usually an array of micropillars) to selectively trap WBCs while allowing the rest of the blood to pass through the device unimpeded (**Figure 1b**). The fundamental disadvantage of dead-end filtration/trapping is that WBCs inevitably plug the filter elements, thus significantly degrading the separation performance over time and limiting the total processed volume. In crossflow filtration, blood flow is directed parallel to the surface of the membrane, and a pressure gradient is established to carry blood cells smaller than the pores across the membrane (**Figure 1c**). Crossflow filtration is therefore significantly less sensitive to clogging because WBCs accumulating on the surface of the membrane are continuously swept away by the blood flowing tangentially to the membrane.

Alvankarian *et al.* implemented the dead-end filtration approach using U-shaped arrays of square pillars to separate WBCs from WB[53]. Fabricated out of polyurethane methacrylate (PUMA) resin, these arrays had a gap of ~5.5 µm between the pillars, which trapped WBCs but allowed RBCs and PLTs to flow through the structure unobstructed. The efficiency of RBC removal (percent of input RBCs that passed through the array) ranged from 84 to 89% at flow rates of 15-50 µL/min (0.015-0.050 mL/min). However, the average WBC separation efficiency (percent of input WBCs trapped in the array) was only 25% at 15 µL/min and was further reduced to ~18% at 50 µL/min.

© SIMTIPRO Srl

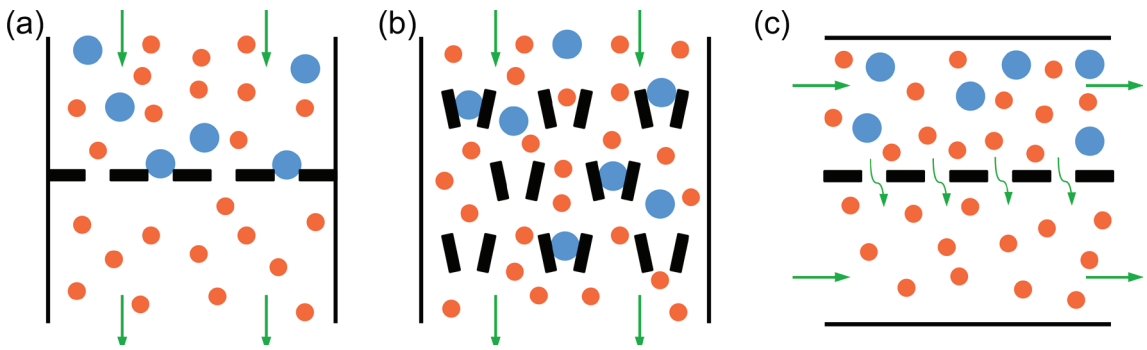

Figure 1 - Filtration through porous membranes and micropillar arrays
(**a**) Dead-end filtration: the blood sample flows perpendicular to the surface of the membrane with pores smaller than the size of WBCs (blue), which are retained by the membrane. (**b**) Microfluidic trapping: microfabricated filter elements selectively trap WBCs while allowing smaller cells (red) to pass through the structure freely. (**c**) Crossflow filtration: the blood sample flows parallel to the surface of the membrane, and a pressure gradient is established to carry blood cells smaller than the pores across the membrane. Green arrows indicate the direction of flow.

Blood Transfus 2023; 21: 494-513 doi: 10.2450/BloodTransfus.506

Table I - *Performance characteristics of microfluidic cell separation technologies*

	Input sample	Input sample HCT (%)	Anticoagulant	Dilution buffer, buffer:sample (v/v)	Sheath buffer, buffer:sample (v/v)	Sample processing rate (mL/min)	WBC removal (%)	RBC loss (%)	Platelet loss (%)	Cell viability (%)	Total volume processed (mL)	Mode of operation
Filtration through porous membranes and micropillar arrays												
Alvankarian *et al.*, 2013[53]	WB	39-52[a]	K2EDTA	None	None	0.015-0.050	18-25	11-16	Not quantified	Not quantified	0.004	Flow-through
Li X. *et al.*, 2014[58]	WB (porcine)	33-48[b]	Not reported	None	PBS, 20:1	(i) 0.008 (ii) 0.017	(i) ~46 (ii) ~27	<1	Not quantified	~97	0.1	Flow-through
Cheng *et al.*, 2016[55]	WB	39-52[a]	K2EDTA	PBS, on chip dilution 10:1	None	0.0375	~72	0.3	Not quantified	Not quantified	0.3	On-chip recirculation, flow-through
Guo *et al.*, 2017[59]	WB	45	EDTA	None	PBS + 0.2% F-127, >2:1	~8.3×10^{-5}	98-99	0	Not quantified	Not quantified	Not reported	Flow-through
Kuan *et al.*, 2018[54]	WB	39-52[a]	K2EDTA	None	PBS, 10:1	0.3×10^{-3}	2.5-4	Not quantified	Not quantified	Not quantified	0.006	Flow-through
Separation due to inertial forces acting on cells in fluid flowing through microchannels												
Wu L. *et al.*, 2012[70]	WBCs + RBCs resuspended in buffer	0.5-2	Sodium Heparin	PBS + 0.5% BSA	None	0.8	98-89%	5-16%	Not quantified	>98	20	Flow-through
Nivedita *et al.*, 2013[71]	WB	0.1	Not reported	0.9% saline	None	1.8	~95	~6	Not quantified	Not quantified	Not reported	Flow-through
Wu Z. *et al.*, 2016[51]	WB	0.10-0.26[a]	Not reported	PBS	None	0.15	75-90	0.2-2	Not quantified	Not quantified	Not reported	Flow-through
Zhang *et al.*, 2017[72]	WB	2-3[a]	Lithium heparin	PBS	None	4.8	>90	<1[c]	<1[c]	Not quantified	Not reported	Flow-through, cascade
Zhou *et al.*, 2018[73]	WB spiked with HepG2 cells	22.5	Not reported	Saline, PBS	Saline, 1:1	0.113	Not reported, 82% for HepG2	2.9%	Not quantified	Not quantified	~2	Flow-through
Zhou *et al.*, 2019[74]	WB	39-5[2]a	Not reported	None	PBS, 2:1	0.133	Not quantified	Not quantified	Not quantified	Not quantified	Not reported	Flow-through
Jeon *et al.*, 2020[75]	WB	0.08-0.10	Heparin	PBS	None	9.2	~80	<0.1	~1	Not quantified	~25	Flow-through, on-chip cascade and recirculation

[a]Estimated based on a normal range for humans[101]; [b]Estimated based on normal range for pigs[102]; [c]Estimated based on the flow cytometry data provided in the study; [d]Residual samples from the leukoreduction system (LRS) chambers of an apheresis machine after routine donor plateletpheresis procedures; [e]Isotonic elutriation buffer comprising 50% Plasmalyte A and 50% of a 0.45% NaCl solution containing 1% BSA, 1.0 mM N-acetylcysteine, and 2% dextrose.

continues on next page

©SIMTIPRO Srl

Table I - *Performance characteristics of microfluidic cell separation technologies (continued from previous page)*

	Input sample	Input sample HCT (%)	Anticoagulant	Dilution buffer, buffer:sample (v/v)	Sheath buffer, buffer:sample (v/v)	Sample processing rate (mL/min)	WBC removal (%)	RBC loss (%)	Platelet loss (%)	Cell viability (%)	Total volume processed (mL)	Mode of operation
Separation using deterministic lateral displacement in micropillar arrays												
Civin *et al.*, 2016[80]	WB	20-26[a]	Not reported	PBS + 5mM EDTA + 1% BSA or P-188	PBS + 5mM EDTA + 1% BSA or P-188, 1:1	0.011	88	0.015	Not quantified	Not reported	0.2	Flow-through
Mutlu *et al.*, 2017[81]	WB	20-26[a]	ACD	PBS + 1% F-127	PBS + 1% F-127, ~4.6:1	~4.4	95.7-96.6	0.0047-0.0059	Not quantified	94.9-99.6	800	Flow-through
Yamada *et al.*, 2017[82]	WB	20-26[a]	ACD-A	PBS + 0.2% BSA	PBS + 0.2% BSA, 2:1	0.04	>90	<5	Not quantified	Not quantified	1.2	Flow-through
Campos-González *et al.*, 2018[83]	LRS samples[d]	10-13[a]	ACD-A	PBS + 0.5% F-127 or 1% BSA, or elutriation buffe[e]	PBS + 0.5% F-127 or 1% BSA, or elutriation buffer, 1:1	~1.167	~80	3	17	96	~15	Flow-through
Separation by leveraging cell-cell interactions in microfluidic channels												
Kim *et al.*, 2016[80]	WB	39-52[a]	EDTA	None	None	0.15	80	Not quantified	Not quantified	99.8	1	Flow-through, on-chip cascade
Separation by skimming off streamlines												
Strachan *et al.*, 2019[96]	MNC leukapheresis	5	ACD-A	PBS + 0.8% P188	None	30	>85	<20	<20	>98	60	Flow-through
Lezzar *et al.*, 2022[97]	WB	10	ACD-A	Normal saline	None	10	>85	10-15	10-15	Not quantified	680	Recirculation

[a]Estimated based on a normal range for humans[101]; [b]Estimated based on normal range for pigs[102]; [c]Estimated based on the flow cytometry data provided in the study; [d]Residual samples from the leukoreduction system (LRS) chambers of an apheresis machine after routine donor plateletpheresis procedures; [e]Isotonic elutriation buffer comprising 50% Plasmalyte A and 50% of a 0.45% NaCl solution containing 1% BSA, 1.0 mM N-acetylcysteine, and 2% dextrose.

©SEETIPRO SRL

This decline was likely due to higher flow rates increasing the pressure gradient across WBCs stuck in the pillar arrays, causing the cells to deform more and thus escape through the gaps between the pillars. Furthermore, the use of undiluted WB led to rapid obstruction of the pillar arrays, thus severely limiting the capacity and separation efficiency of the device[53].

To circumvent the adverse effects of pore clogging seen in dead-end filtration, Li *et al.* designed a crossflow filtration device[58]. Made of polydimethylsiloxane (PDMS), the device consisted of two microfluidic channels separated by a microfiltration membrane (also made of PDMS) with 4 μm pores. A stream of blood sample and a stream of phosphate buffered saline (PBS) buffer (sheath flow) were injected into the top channel in such a way that the sheath flow forced the blood cells through the membrane. Cells larger than the pore size (e.g., WBCs) remained above the membrane and were collected with the sheath buffer from the top channel. Smaller cells (e.g., RBCs) passed through the membrane pores and were collected from the bottom channel outlet. When processing porcine WB at a flow rate of 0.5 mL/hr (0.008 mL/min) with a sheath buffer flow rate of 10 mL/hr, the device demonstrated WBC separation efficiency of 46.4±1.8% and WBC purity of 65.2±5.1%. At a higher flow rate of 1 mL/hr (0.017 mL/min) with a sheath buffer flow rate of 20 mL/hr, the WBC separation efficiency decreased to 27±4.9% but WBC purity increased to 93.5±0.5%. The viability of separated WBCs was ~97% for either flow rate and there was no significant difference in viability of WBCs before and after the separation. The crossflow filtration design, the high porosity, and the large surface area of the microfiltration membrane significantly extended the clog-free operation of the device; in experiments with microbeads, no signs of clogging were observed within the first 30 minutes[58].

Similar to Li *et al.*[58], Cheng *et al.*[55] developed a cross-filtration device that comprised two microfluidic channels stacked on top of each other and separated by a microporous membrane[55]. In this case, however, the embedded membrane was made of polycarbonate and featured smaller 3 μm pores. Furthermore, the device incorporated a rotatory micropump which was used to circulate the sample within the chip. Prior to separation, the device was filled with PBS buffer and then loaded with a 300 μL sample of WB. The sample was driven through the membrane to filter out RBCs and PLTs, and then the flow was reversed to flush out WBCs trapped within the pores. The flow rate within the device was limited to 545 μL/min as faster flow rates increased the pressure drop across the membrane, increasing WBC deformation and allowing the cells to squeeze through the pores and escape with the filtrate[53,55]. Additional buffer (for a combined total of ~3 mL of PBS) was continuously introduced during the procedure to help wash out RBCs and PLTs. The filtration/reverse flushing cycle was repeated five times, resulting in a WBC recovery of ~72%, RBC removal of 99.7%, and an effective sample processing rate of 37.5 μL/min (0.0375 mL/min) i.e. taking 8 minutes to process 300 μL[55].

A device developed by Guo *et al.* used an anisotropic filter created by an array of specially designed micropillars and a combination of crossflow and oscillatory flow patterns to separate WBCs from WB[59]. The device consisted of an array of micropillars designed to shape the inter-pillar gaps as funnels. The effective pore size of the funnels in each row decreased from 8 μm at the bottom to 2 μm at the top of the array. An oscillatory flow pattern directing cells in (from bottom to top) and out (from top to bottom) of the funnels was superimposed over the crossflow directed from left to right in the device. During the separation, a sample of undiluted WB was injected at the bottom left conner of the array. Deformable RBCs were able to pass through the successively narrowing funnels moving generally toward the top right conner of the array. WBCs became stuck in the funnels and were released when the oscillatory flow was reversed, allowing them to be swept toward their respective outlets by the tangential crossflow. The device demonstrated a WBC separation efficiency of >98% with 100% purity (no RBC contamination), but at a flow rate of only ~5 μL/hr (8.3×10^{-5} mL/min). Although no cell viability measurements were done, the authors postulated that the deformations experienced by the cells were too small to have any effect on viability[59].

Finally, Kuan *et al.*[54] combined crossflow filtration with the so-called "plasma skimming" effect, which occurs at vessel bifurcations (where the daughter branch with the highest flow receives a disproportionately larger fraction of blood cells)[60,61], to separate WBCs from RBCs and plasma[54]. This device consisted of two inlet channels (for injecting WB and sheath buffer) that converged into a straight segment

© SIMLIPRO Srl

featuring a series of branches on one side for extracting plasma and RBCs and connected to a massive array of rectangular and triangular pillars designed for capturing WBCs. During the separation, a 6 µL sample of WB passing through the device at 0.3 µL/min (0.3×10^{-3} mL/min) was pushed by the sheath flow (PBS at 3 µL/min) toward the side branches to enhance the extraction of plasma and RBCs. The flow of WB sample mixed with the sheath buffer was directed into the pillar array for WBC trapping. The device isolated 1,200-1,800 WBCs from 6 µL of WB, which equates to WBC removal of ~2.5-4% (assuming a normal WBC count of 7,500-8,000/µL)[62,63]. Analyses of the extracted plasma suggested minimal hemolysis. Furthermore, clogging was reduced by incorporating large gaps between each subsequent row of pillars[54].

Microfiltration-based microfluidic devices show a significant potential for enabling leukapheresis applications because minimal or no dilution is required to work with WB. Additionally, high levels of WBC separation efficiency have been achieved in several recent designs. However, the flow rates demonstrated so far remain very low, and inherent plugging reduces WBC separation performance over time, limiting the ability of the devices to process large volumes of blood. Multiplexing to increase the overall flow rate and novel approaches to counteract plugging (like the ones described by Cheng *et al.*[55] and Guo *et al.*[59]) could potentially help overcome these shortcomings.

Separation due to inertial forces acting on cells in fluid flowing through microchannels

Blood cells flowing in suspension through microfluidic channels experience a combination of the shear-induced lift force (F_S), which pushes the cells toward the walls of the channel, and the wall-induced lift force (F_W), which pushes the cells toward the centerline of the channel (**Figure 2a**). The interplay between these two inertial forces results in the lateral migration of the cells across the channel cross-section to equilibrium positions determined by cell size, channel geometry, and flow rate[64-67]. In curved channels, fluid experiences centrifugal acceleration under a combination of viscous and inertial forces, which leads to the formation of two counter-rotating Dean vortices in the upper and lower halves of the channel cross-section. These vortices are responsible for exerting the Dean drag force (F_D) on the cells (**Figure 2b**). A cell's position in the cross-section of a curved rectangular microfluidic channel is determined by the ratio of the sum of the lift forces to the Dean force and is proportional to the cell diameter (d), $(F_S+F_W)/F_D \propto d^3$. As a result, smaller cells become entrained in the Dean flow more than larger cells which tend to remain closer to the equilibrium positions defined by the balance of the lift forces. In a rectangular channel with a width much larger than height, this phenomenon leads to WBCs positioning closer to (and RBCs and PLTs further away from) the wall of the channel nearest to the center of the curvature[66,68,69].

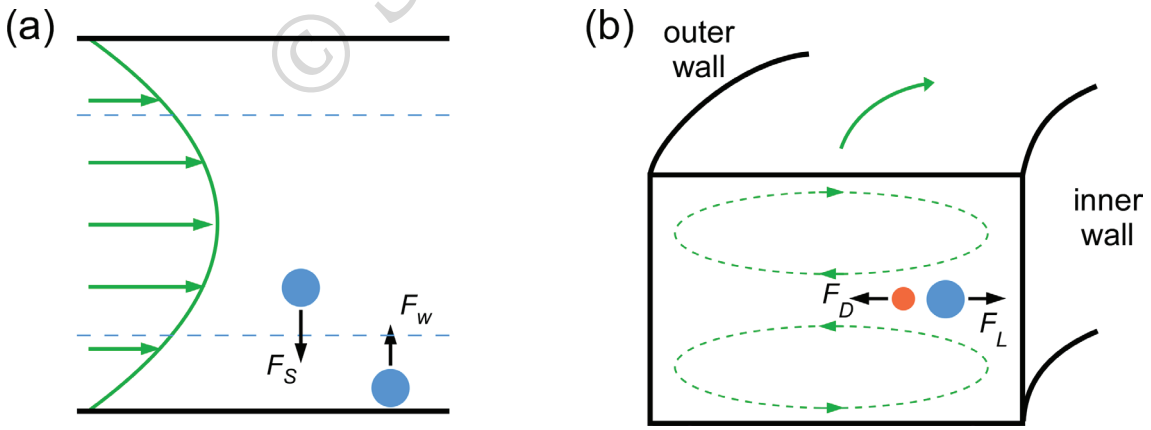

Figure 2 - Separation due to inertial forces acting on cells in fluid flowing through microchannels
(**a**) Cells flowing in a microfluidic channel experience the shear-induced lift force (F_S), which pushes the cells toward the channel walls, and the wall-induced lift force (F_W), which pushes the cells toward the channel centerline. The interplay between these two inertial forces results in the lateral migration of cells within the channel cross-section to equilibrium positions that depend on cell size. (**b**) Fluid flow in curved microchannels generates two so-called Dean vortices counter-rotating symmetrically in the upper and lower halves of the channel. The balance of the net inertial lift forces (F_L) and the Dean drag force (F_D) determines each cell's position in the channel cross-section in a size-dependent fashion.

© SIMTRO Srl

A major challenge when using spiral channels for separating blood cells is confining the vast number of RBCs present in WB to their equilibrium position defined by the inertial forces. The ubiquitous cell-cell interactions, particularly at higher HCTs, de-focus and expand the RBC band to overlap with the equilibrium position of WBCs. To address this issue, Wu L. *et al.* developed a separation device with a spiral channel of a trapezoidal cross-section (the outer wall taller than the inner wall) to change the geometry of the Dean vortexes and shift the equilibrium position of the smaller cells further away from the inner wall[70]. Because of this modification, RBCs formed a band closer to the outer wall (and hence further away from WBCs, which were localized near the inner wall) and in the widest part of the channel (better able to accommodate de-focusing due to cell-cell interactions). The device processed reconstituted mixtures of RBCs and WBCs suspended in PBS buffer containing 0.5% BSA with HCT of the suspension ranging 0.5-2% at flow rates as high as 0.8 mL/min. Depending on sample HCT, WBC recovery was 98-89% and RBC removal was 84-95%. The viability of WBCs was >98% and there was no significant difference in WBC activation before and after separation. The authors postulated that the risk of clogging was minimized by the large dimensions of the microchannels, a consideration common among most of the inertial forces-based devices[70].

Nivedita *et al.* developed a cell separation device that consisted of a spiral rectangular microchannel with an inlet at the center of the spiral and several outlets at the end of the spiral for collecting separated WBCs, RBCs, and PLTs[71]. When passing through the device, blood cells migrated to positions within the channel cross-section according to their size, with WBCs clustering near the inner wall of the channel (the wall closest to the center of the spiral). When processing WB diluted to 0.1% HCT at a flow rate of 1.8 mL/min, the device demonstrated WBC separation efficiency (percent of total output WBCs collected from the WBC outlet) of 95±2.2% and RBC separation efficiency (percent of total output RBCs collected from the two RBC outlets) of 94±2.5%. Platelets failed to separate and were distributed between all outlets[71].

Wu, Z. *et al.* developed an inertial separation device that consisted of a straight rectangular channel with a section containing a series of paired square microstructures protruding symmetrically from the side walls. The gap between the microstructures was kept at 30 µm to minimize the possibility of blood cells clogging the channel. The sudden narrowing/expansion of the channel lumen caused by the microstructures induced localized secondary flows that enhanced the separation[51]. The device was tested with WB diluted with PBS to 0.25-0.5% by volume (0.10-0.26% estimated HCT) at flow rates ranging from 50 to 200 µL/min. The separation performance was maximized at a flow rate of 150 µL/min (0.15 mL/min). For the 0.10% HCT sample, the separation efficiency was 89.7% for WBCs and 99.8% for RBCs (the corresponding purity was 91.0% for WBCs and 99.6% for RBCs). With a higher HCT (0.26%), the separation efficiency declined to ~75% for WBCs and ~98% for RBCs. The authors postulated that their device could be easily multiplexed to increase the overall throughput, but this was not evaluated experimentally[51].

Zhang *et al.* took another unique approach to inertial separation by utilizing a series of U-turns to generate the secondary flows[72]. A device comprising eight such serpentine channels multiplexed in parallel achieved a flow rate of 288 mL/hr (4.8 mL/min) and, when tested with WB diluted 20 times with PBS (2-3% estimated HCT), demonstrated a WBC separation efficiency of >90% and purity of 48.1%. Although not explicitly reported by the authors, the RBC and PLT loss can be estimated from the provided flow cytometry data to be <1%. Furthermore, due to the channels' large width (200 µm) and lack of structural obstructions, there were no clogging issues associated with the device. The authors also suggested that the shear rate was too low to cause any functionality and viability issues for the separated WBCs[72].

Zhou *et al.* combined inertial focusing and shear-induced diffusion with the elastic force at the interface between Newtonian (buffer) and non-Newtonian (WB) fluids in a co-flow system to separate blood cells by size[73,74]. Their device consists of a straight rectangular microchannel in which a stream of buffer is flanked on either side by two streams of diluted WB. The authors postulated that cells first migrate from the WB streams toward the buffer stream under the influence of the shear-induced diffusion and the elastic force, and then continue to migrate within the buffer stream toward the channel centerline due to the inertial forces. Because larger cells migrate faster

© SIMTIPRO Srl

than smaller cells, WBCs accumulate preferentially in the central buffer stream[73,74]. In their earlier work, a sample of WB diluted with saline or PBS down to 22.5% HCT was spiked with Hep G2 cells and perfused through the device at a flow rate of 112.5 µL/min (0.133 mL/min), with the buffer flow rate also at 112.5 µL/min. As a result, the buffer stream outlet contained 89.1% of the Hep G2 cells and 2.9% of the RBCs initially present in the input sample; separation efficiency for WBCs or PLTs were not reported[73]. In a follow-up study, the device was tested by processing a sample of WB at a flow rate of 133 µL/min (0.133 mL/min), with the flow rate of the buffer being 267 µL/min. WBCs migrated into the buffer stream faster than RBCs and hence their relative frequency increased by about 2.6-fold. However, no additional information on the device separation performance for WBCs, RBCs and PLTs was provided[74].

Finally, Jeon *et al.* developed a multi-dimensional double spiral (MDDS) device comprising two different spiral channels connected serially. In this two-stage design, the first spiral channel had smaller dimensions and a rectangular cross-section to perform general focusing of the cells in the sample. The second spiral channel had larger dimensions and a trapezoidal cross-section to enhance the separation of cells by size[75]. When tested with a sample of WB diluted 1:500 with PBS, the MDDS device operating in the flow-through regime demonstrated a WBC recovery of >95%, while removing >92% of RBCs at a flow rate of 2.3 mL/min. Further, the authors presented a multiplexed device comprising eight MDDS units which also incorporated a built-in check-valve to recirculate the WBC-rich output back through the device for additional enrichment and concentration. This version of the device could operate at flow rates as high as 18.4 mL/min; however, best separation results were obtained at 9.2 mL/min for which recovery of 80% of WBCs with purity of 45% was demonstrated, while removing >99.9% of RBCs and ~99% of PLTs. Flow cytometry analysis showed no significant cell activation despite the relatively high flow rate[75].

Overall, separation devices utilizing inertial forces hold great promise because of the considerable flow rates and excellent separation efficiencies demonstrated in recent studies. Additionally, these devices have simple designs that could be relatively straightforward to fabricate commercially for eventual clinical trials. However, a significant drawback is that most of these devices require significant dilution of WB to operate efficiently. Therefore, a leukapheresis platform based on inertial focusing technology will likely need to incorporate hemodilution before and hemoconcentration after passing through the device to be useful in the clinical setting.

Separation using deterministic lateral displacement and other similar methods in micropillar arrays

Deterministic lateral displacement (DLD) technology utilizes arrays of pillars to separate cells based on size. Unlike microfluidic filtration or trapping, the gaps between the pillars in a DLD array are larger than the cells and therefore present no physical hindrance to their movement. Instead, the geometry of the pillar arrays is used to manipulate the streamlines in such a way as to predetermine the path of cells depending on the relationship between the cell size and streamline width[76-78]. In a classical DLD array, the subsequent rows of pillars are shifted relative to one another to effectively split the flow passing through a gap in one row and direct a streamline of a certain width to pass on the other side of the pillar in the next row. As a result, cells with an effective radius smaller than the streamline width follow the streamline zig-zagging through the array, while larger cells are "bumped" by the pillars and shift laterally further with each row (**Figure 3**)[76]. This effective size cutoff (known as the "critical diameter") depends on the geometry of the DLD array, including the gap size, pillar size and shape, and the degree of row shift[79].

Civin *et al.* developed a WBC separation device with a DLD array that consisted of three distinct zones that featured critical diameters progressively decreasing in size (8 µm, 5.5 µm, and 4 µm)[80]. The design included a central channel carrying a stream of buffer flanked by two mirror images of the DLD array on either side carrying blood sample streams; the flow rate ratio between the two fluids was ~1:1. These two arrays "bumped" WBCs into the central stream, which was ultimately collected through a product outlet. Smaller cells (RBCs, PLTs) continued following the initial flow direction toward the downstream waste outlets. The device was tested using WB diluted 1:1 by volume (estimated HCT of 20-26%) with the run buffer that consisted of PBS with 5 mM EDTA and 1% of either BSA or Poloxamer 188 solution (P-188). The device was able to process the diluted WB sample at ~0.011 mL/min

© SIMTIPRO Srl

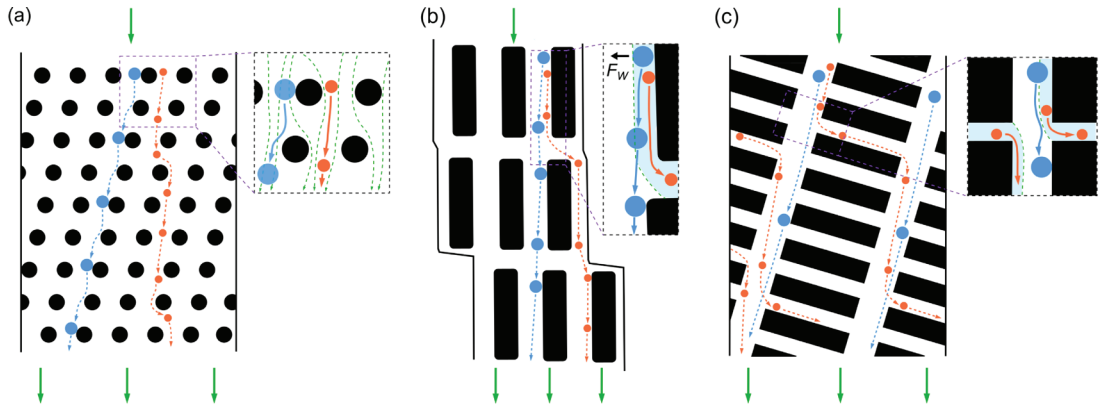

Figure 3 - Separation using deterministic lateral displacement and similar methods in micropillar arrays
(**a**) Each subsequent row of pillars in a classical DLD array is shifted relative to the previous row to split the flow passing through the inter-pillar gap in one row and direct a streamline of a certain width to pass on the other side of the pillar in the next row. Because the effective radius of WBCs (blue) is larger than the streamline width, they are "bumped" by the pillars displacing laterally further with each row. RBCs and platelets (red) follow the streamline zigzagging through the array. (**b**) The lateral displacement of WBCs can be enhanced by taking advantage of the wall-induced lift force (F_w) experienced by the cells flowing near rectangular pillars elongated in the direction of flow. (**c**) The degree of separation between WBCs and RBCs can be enhanced by extending the pillars laterally to make the smaller cells travel further within the device after each streamline splitting bifurcation.

(200 µL in ~18 minutes), recovering on average 88% of WBCs and removing on average >99.985% of RBCs. The authors minimized the possibility of clogging by filtering all blood samples through a 20 µm filter prior to introduction into the device[80].

Mutlu *et al.* enhanced the traditional DLD design by taking advantage of the strong dependence of the inertial lift forces on the size of cells flowing near rectangular pillars that were elongated in the direction of flow[81]. In their design, a stream of blood and a stream of buffer were pumped through a DLD array of elongated pillars. Smaller cells (RBCs, PLTs) followed the streamlines to remain within the bloodstream, while larger WBCs migrated toward the buffer stream under the combined influence of the DLD bumping and the wall lift force. Multiplexing 104 devices in parallel allowed for the processing of diluted WB (1:1 dilution with PBS containing 1% F-127, an estimated HCT of 20-26%) at ~4.4 mL/min (800 mL over ~3 hours) with 95.7-96.6% WBC recovery, 0.0047-0.0059% RBC loss, and 94.9-99.6% WBC viability. In these large volume experiments, the ratio of the buffer flow rate to the blood sample flow rate was ~4.6:1 and no clogging was observed for entire duration of the separation procedure[81].

Yamada *et al.* made another novel modification of the classical DLD array by extending the pillars laterally to effectively create a lattice composed of "main channels" (slanted against the macroscopic direction of flow at a fixed angle ranging from 15-45°) and "separation channels" (crossing the main channels at a 90° angle)[82] . The density of separation channels was 30-100 times greater than that of the main channels, producing an asymmetrical flow distribution at each bifurcation. The device had three inlets (for injecting a stream of blood flanked by the streams of buffer on either side) and six outlets (for collecting cells of different sizes). Cells that were larger than the width of the streamline entering the separation channels were "bumped" at each bifurcation to continue along their initial path through the main channels. Smaller cells entered the separation channels and followed the characteristic zip-zag motion through the lattice away from the larger cells. When processing WB diluted 1:20 with PBS containing 0.2% BSA (an estimated HCT of 2.0-2.6%) at a flow rate of 40 µL/min (0.04 mL/min), with the flow rates of the two buffer streams being 30 and 50 µL/min, the device removed >90% of WBCs with an RBC loss of <5%. There was no clogging observed during a 30 min operation of the device. The authors also described a multiplexed device comprising eight individual lattice devices arranged in parallel that operated at a sample flow rate of 0.4 mL/min, but this device has yet to be tested with blood[82].

Campos-González *et al.* used the same classical DLD design as Civin *et al.*[80] to develop a device for separating WBCs for cellular therapy applications[83]. The device consisted of 14 DLD arrays multiplexed in parallel and was tested using samples of concentrated mononuclear cells (MNCs) recovered from the leukoreduction system (LRS)

© SIMLIPRO SRL

chambers of an apheresis machine after routine donor plateletpheresis procedures. These samples had RBC counts similar to WB, but they contained virtually no granulocytes and had a much higher count of MNCs (10-20-times) and PLTs (10-times) than in a typical WB sample. To test the separation performance of the device, the LRS samples were diluted 1:4 with either PBS, containing 0.5% F-127 or 1% BSA, or an isotonic elutriation buffer, containing 1.0% BSA (an estimated HCT of 10-13%). The device recovered, on average, ~80% of WBCs while removing ~97% of RBCs and >83% of platelets at a sample flow rate of 1.16 mL/min. The viability of cells after the separation was 96%[83].

Overall, the separation devices based on DLD require minimal WB dilution, demonstrate excellent separation efficiencies, and can operate at substantial flow rates when multiplexed. These characteristics make DLD-based devices highly competitive as candidates for replacing centrifugation-based methods in many cell separation scenarios. However, producing DLD arrays requires precise microfabrication technique and processing that may not be readily available to commercial manufacturers. Moreover, operating these devices requires multiple pumps and an associated control system to precisely balance and maintain the streams of buffer and blood within the device. These significant challenges must be addressed before DLD technologies become suitable for leukapheresis applications.

Separation by leveraging cell-cell interactions in microfluidic channels

Cell-cell interactions cause WBCs to separate from RBCs when flowing through the microvascular networks *in vivo*[84,85]. Many of these naturally occurring phenomena can be mimicked in microfluidic channels *in vitro* and subsequently utilized for the purposes of cell separation[60,61]. For example, the formation of "comet tails" (the densely packed RBC trains forming behind individual WBCs as they traverse narrow capillary microchannels) can be used for efficiently capturing WBCs into microfabricated sprouts[86]. The natural microcirculatory phenomena can also be artificially enhanced by manipulating the geometry of microfabricated capillaries[87]. For example, rectangular microchannels with a low aspect ratio cross-section make WBC margination (the lateral migration of WBCs towards the vessel wall induced by RBCs interactions) particularly effective at separating WBCs from the rest of the blood (**Figure 4a**)[60,88]. Because these natural phenomena are driven by RBC-WBC interactions, the separation process is notoriously probabilistic, and therefore, several separation units may need to be cascaded to increase efficiency. Using this approach, a microfluidic device comprising a series of repeated expansions and contractions of a straight microchannel (to mimic RBC-induced margination of WBCs in post-capillary venules) can separate WBCs from WB with high efficiency[89].

© SIMIPRO Srl

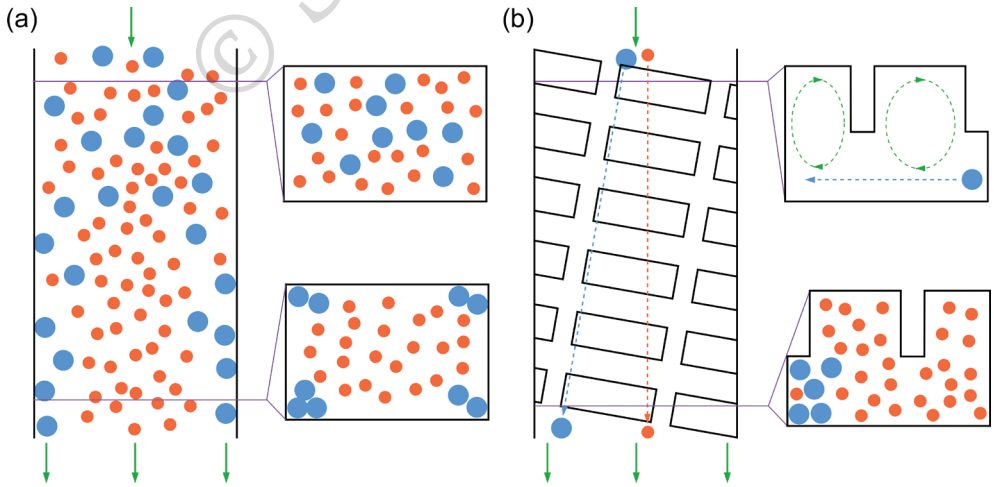

Figure 4 - Separation by leveraging cell-cell interactions
(**a**) When flowing with WB at physiologic HCT in rectangular microchannels, WBCs (blue) migrate laterally toward the channel walls (marginate) due to the cell-cell interactions with RBCs (red). (**b**) The efficiency of WBC separation using margination can be significantly enhanced in a rectangular microfluidic channel with a classical hydropheresis design, such as having an array of rectangular "pits" built into one of the channel walls.

Kim *et al.*[90] used the geometrical configuration of their device's features to amplify the natural RBC-WBC interactions to separate WBCs from WB[90]. Their device consisted of a linear microfluidic channel with a rectangular cross-section and a slanted array of discontinuous rectangular "pits" built into its top wall, similar to a typical hydrophoresis design (**Figure 4b**)[91]. Unlike in hydrophoresis, however, the displacement of WBCs was driven by their interactions with RBCs that tended to occupy the pits at physiologic levels of HCT (rather than by collisions with the walls of the features). Pushed outwards by the RBCs, WBCs migrated towards one of the sidewalls of the main microchannel, driven by the secondary transverse flows generated by the pit array[90]. Four devices were multiplexed in series to improve the purity of WBC separation. When tested with undiluted WB, the multiplexed device was able to separate WBCs with 80% recovery, 10.4% purity, and 99.8% viability, while operating at 150 µL/min (0.15 mL/min)[90].

Overall, methods that rely on interactions between WBCs and RBCs tend to work best at physiologically high levels of HCT, which is a unique advantage of these methods. Because no buffer is used in any part of the separation process, the separated RBCs and PLTs could be returned to the patient, without any postprocessing. However, because the separation efficiency decreases for lower HCTs, these methods may not work as well for anemic patients. Additionally, the separation channels often need to be relatively small to take maximal advantage of the cell-cell interactions and several separation units need to be cascaded in series to increase the purity and yield. Narrow, shallow, or lengthy channels increase the fluidic resistance of the device, which ultimately limits the flow rate at which the separation can be performed. Nevertheless, the WBC separation methods based on cell-cell interactions hold great promise for use in leukapheresis applications either as stand-alone devices or as part of a hybrid platform.

Separation by skimming off streamlines

A diverse group of microfluidic cell separation methods operate by skimming off streamlines of a certain width from the main flow and diverting them away through a series of side channels (**Figure 5**)[50,57,92]. Cells that are smaller than the streamline width follow the streamlines into the side-channels, and those that are larger continue with the main flow. In a sense, these methods implement "plasma skimming", a natural microcirculatory phenomenon occurring at uneven capillary bifurcations *in vivo*, where the daughter branch with the fastest flow receives most of the cells entering the bifurcation[60,61,93]. The cell size cutoff is determined by the width of the extracted streamlines, not the dimensions of the side-channels, which is the fundamental difference between these innovative designs and the classical filtration methods discussed earlier. Unlike the DLD-based designs, the "skimming" methods divert the smaller cells extracted with the streamlines into the side channels and thus completely avoid back mixing caused by reintroducing separated cells into the main flow[92,94,95].

Strachan *et al.* utilized these concepts using the "controlled incremental filtration" (CIF) approach[94,95] to enrich WBCs from MNC leukapheresis samples[96]. Following a typical CIF design, their device consisted of a central channel separated from two side channels on either side by a series of pill-shaped pillars[96]. Every two sequential pillars defined a filtration gap through which a small fraction of the central channel flow was extracted into the corresponding side channel (**Figure 5**). The geometry of the pillars and gaps remained the same, while the widths of the side and central channels changed along the length of the device to accommodate the redistribution of flow. The changes in widths of the central and side channels were iteratively calculated and adjusted to maintain a constant width of the streamline extracted through each subsequent gap along the length of the device. Cells smaller than the size cut-off defined by the streamline width (i.e., RBCs and PLTs) were carried by the extracted fluid into the side channels, while larger cells (i.e., WBCs) remained in the central channel and were collected with the retentate. Forty-eight of such CIF devices multiplexed in parallel processed the MNC leukapheresis samples with minimal or no dilution required at flow rates ranging from 4 mL/min (gravity-driven flow) to 50 mL/min (flow driven by a syringe pump). At 30 mL/min, the multiplexed device removed >85% WBCs with >98% viability, while losing about 20% of RBCs and PLTs[96].

More recently, Lezzar *et al.* tested whether a CIF-based device could be used for separating WBCs from blood in the recirculation regime[97]. The device comprised 48 CIF elements multiplexed in parallel with an overall design

© SIMTIPRO Srl

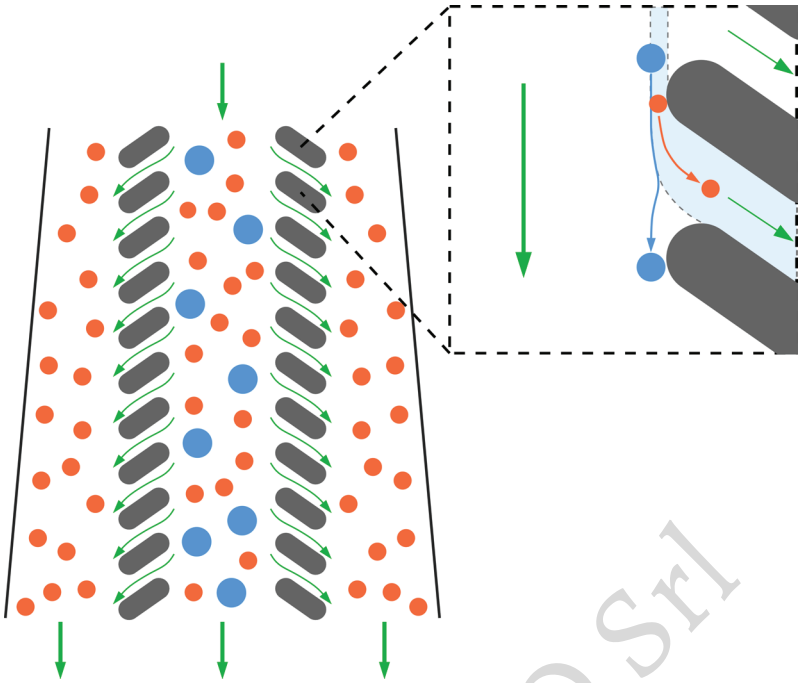

Figure 5 - Separation by skimming off streamlines
A typical design consists of a series of side channels, each diverting a streamline of a certain width away from the flow in the main channel. Cells smaller than the streamline width (e.g., RBCs) follow the streamlines into the side channels, and those that are larger (e.g., WBCs) continue to flow in the main channel.

© SIMTIPRO Srl

similar to Strachan *et al.*[96]. The CIF device was tested using samples of WB with HCT adjusted from 5 to 30% by dilution with normal saline and at flow rates ranging from 10 to 30 mL/min. In the flow-through regime, the separation performance of the device was maximized (>85% WBC separation efficiency, <15% RBC and PLT loss) for WB samples with 10% HCT at a flow rate of 10 mL/min. For WB with 20% HCT, the CIF device removed ~60% of the WBCs passing through the device, while similarly minimizing the loss of RBCs and PLTs. When tested in the recirculation regime with the optimal parameters (10% HCT, 10 mL/min flow rate), the device demonstrated a similar level of separation performance, virtually depleting WBCs in the recirculating blood (~98% reduction) by the end of a 3.5-hour simulated leukapheresis procedure. The device operated without clogging or any noticeable decline in separation performance during recirculation. Although WBC viability was not measured, an extensive analysis revealed that the device did not increase the activation of WBCs and PLTs above a benchtop control and caused no measurable damage to RBCs[97].

Microfluidic devices utilizing CIF for blood cell separation hold great promise because of a particularly favorable combination of high separation efficiencies and flow rates that can be achieved for concentrated suspensions of blood cells. CIF is also the only microfluidic cell separation technology for which operation in the recirculation regime has been successfully demonstrated to date. Recent studies have shown that these devices are capable of processing large volumes of blood (>600 mL) over extended periods of time (hours) without clogging nor decline in separation performance. Additionally, CIF-based technologies maintain a high viability of separated WBCs with minimal activation and no noticeable damage to cells in recirculating blood. However, further research is needed to fully ascertain whether CIF-based devices could separate WBCs from patient blood with sufficient volumetric throughput and high separation efficiency to ultimately enable centrifugation-free leukapheresis.

CHALLENGES AND OPPORTUNITIES AHEAD

Microfluidic cell separation has undergone a transformative advancement in the last decade. Many of the design milestones for enabling microfluidic leukapheresis have been achieved by at least some of

the technologies. For example, a recent study from our laboratory demonstrated efficient separation of WBCs in the recirculation regime, with RBCs and PLTs returned undamaged to a blood bag meant to simulate the TBV of a pediatric patient[97]. Several of the recently reported devices demonstrated flow rates ranging from 5 to 50 mL/min, although higher flow rates were typically associated with lower separation performance. This negative association, however, was often due to device deformation rather than any fundamental limitations of the microfluidic separation methods[81,96,97]. Our recirculation study[97], as well as other reviewed studies that tested their cell separation devices in the flow-through regime[81,83,96], have also shown the feasibility of processing large volumes (>100-600 mL) of minimally diluted WB with no significant clogging or performance issues. In general, the microfluidic cell separation preserved the viability of separated WBCs, had a minimal effect on PLT activation, and did not cause hemolysis[97]. However, very few studies comprehensively evaluated the effect of processing on PLTs and RBCs, likely because their original research focus was on WBC isolation rather than the preservation of RBC and PLT function. Reporting the effect of microfluidic cell separation on RBCs and PLTs would be particularly important when studying methods that require shifting the cells into a stream of a buffer as part of the separation[54,58,59,73,80-83] or rely on small features as narrow/shallow channels represent notoriously high shear environment[54,55,58,59,80]. The narrow focus on maximizing WBC isolation was also likely the reason why most of the reviewed studies used anticoagulants (e.g., K2EDTA) and dilution buffers (e.g., PBS with BSA and/or various poloxamers) that are incompatible with the current leukapheresis practice. More recent publications have shown that microfluidic cell separation devices can function equally well when using FDA-approved anticoagulants (e.g., ACD-A, Heparin) and buffers (e.g., normal saline)[81,83,97].

Furthermore, even with significant multiplexing, microfluidic devices have naturally small void volumes. For example, the void volume of the CIF device described in our recent study was 0.4 mL (excluding connecting tubing)[97]. Even if microfluidic channels were to occupy the entire footprint of the assembled device (~10 cm in diameter), its void volume would still be only ~1.1 mL, a volume >100-times less than that of the smallest collection set used by centrifugation-based leukapheresis machines. Therefore, the desired reduction of ECV to <10% of a patient's TBV (e.g., to <80 mL for a 10 kg infant) would be eminently achievable for virtually any microfluidic cell separation method discussed in this review.

Significant challenges common to all microfluidic cell separation devices remain, including improving the efficiency of separation at physiologic levels of HCT and demonstrating separation for samples with elevated WBC counts. Although some of the reviewed microfluidic technologies work with undiluted WB, their separation performance decreases significantly for higher flow rates[53,54,58,59,74,90]. Therefore, a substantial degree of multiplexing must be utilized to reach the relevant level of volumetric throughput for these methods. Several cell separation devices based on DLD and CIF technologies have shown excellent separation performance with WB diluted to 5-20% HCT[81,83,96,97]; after some additional design improvements, these devices will likely be able to process WB samples with HCT as high as 15-20% (which may already be acceptable for some patients). Pediatric patients undergoing leukodepletion are severely anemic (~20-25% HCT)[43,44], and those undergoing leukapheresis for cellular collection are moderately anemic (~30% HCT)[30,46-48]. During leukapheresis, the HCT of WB is further reduced due to dilution with saline that is used to prime the extracorporeal circuit (<10% of patient's TBV) and the citrate-based anticoagulant that is continuously infused during the procedure (a dilution ratio of 1:12 is common). In principle, WB could also be diluted with saline to the appropriate HCT before entering a microfluidic cell separation device, then later concentrated back to the physiologic HCT using a standard hemoconcentrator (e.g., Hemocor HPH Junior, Minntech Corp., Minneapolis, MN, USA) before returning to the patient.

The initial WBC count of pediatric patients who undergo leukodepletion is typically 300-500×10^3/μL, but it can also be as high as 900×10^3/μL[43,44]. The WBC count of pediatric patients who undergo cellular collection can range from 0.5×10^3/μL to 85×10^3/μL[30,46-48]. It is unlikely that a single microfluidic cell separation device could work equally well over the entire range of WBC counts encountered among pediatric patients undergoing leukapheresis.

© SIMTIPRO Srl

Therefore, multiple specialized microfluidic devices (each utilizing a different cell separation method) may have to be developed to fully account for the heterogeneity of patient characteristics and treatment modalities encountered in clinical practice.

The remarkably high WBC separation efficiencies demonstrated in recent studies by several microfluidic devices[81,83,96,97] suggest that the loss of RBCs and PLTs during the leukapheresis procedure could be significantly reduced, minimizing the need for transfusion. Replacing centrifugation-based methods with a more efficient microfluidic cell separation technology would potentially transform the convenience and safety of the leukapheresis in the pediatric setting. The main limitation of performing leukapheresis in young children is the need for large-bore catheters to accommodate the very high flow rates required for conventional centrifugation-based machines. In small patients whose peripheral veins may not be able to accommodate even a 17 Ga rigid needle for blood removal, central venous access is often the only suitable route[98]. Placement of a central venous catheter is associated with significant risks, including catheter-related thromboses, vascular and organ injury, and the need for procedural sedation and ICU care, especially in patients who are not amenable to non-pharmacologic calming interventions (e.g., young children and infants)[99]. Performing leukapheresis with a high-efficiency microfluidic device would allow for the reduction of flow rate during the procedure, thus obviating the need for large-bore catheters and central venous access. In the context of leukodepletion, more efficient removal of WBCs would help reduce the amount of blood that needs to be recirculated and the overall duration of the procedure. Shorter procedures may benefit patients by being safer, more rapidly deployable, and less expensive. This, in turn, may lead to new studies into the use of leukapheresis in the early treatment of ALL and AML since the barriers to the procedure (e.g., need for large bore catheters, delay of chemotherapy initiation) may be abrogated[100]. In the context of the cellular collection, the use of high-efficiency microfluidic cell separation devices could enable isolating a sufficient number of desired cells from a standard 500 mL unit of WB obtained via venipuncture, thus eliminating the need for leukapheresis at least in some patients.

ACKNOWLEDGMENTS

This work was supported in part by the National Heart, Lung, and Blood Institute of the National Institutes of Health under Award Number R01HL151858. The content is solely the responsibility of the Authors and does not necessarily represent the official views of the National Institutes of Health, the U.S. Department of Veterans Affairs, or the United States Government.

AUTHORSHIP CONTRIBUTIONS

This comprehensive review is a result of collaboration between Dr. Shevkoplyas, a biomedical engineer with expertise in microfluidic blood cell separation, and Dr. Lam, a clinician scientist with extensive clinical experience in the practice of leukapheresis as well as its current limitations, especially in pediatric patients. Dr. Shevkoplyas and Dr. Lam have contributed equally to this work.

DISCLOSURE OF CONFLICTS OF INTEREST

SSS is an inventor of U.S. Patent #9,789,235 'Separation and concentration of particles' describing the "controlled incremental filtration" technology, and a co-founder of Halcyon Biomedical Incorporated, a company that would benefit from its commercialization. All other Authors declare no conflict of interest.

© SIMTRO SRL

REFERENCES

1. Maitta RW. Current state of apheresis technology and its applications. Transfus Apher Sci 2018; 57: 606-613. doi: 10.1016/j.transci.2018.09.009.
2. Ganzel C, Becker J, Mintz PD, Lazarus HM, Rowe JM. Hyperleukocytosis, leukostasis and leukapheresis: practice management. Blood Rev 2012; 26: 117-122. doi: 10.1016/j.blre.2012.01.003.
3. Padmanabhan A. Cellular collection by apheresis. Transfusion 2018; 58: 598-604. doi: 10.1111/trf.14502.
4. Lichtman MA, Weed RI. Peripheral cytoplasmic characteristics of leukocytes in monocytic leukemia: relationship to clinical manifestations. Blood 1972; 40: 52-61. PMID: 4504250
5. Lichtman MA, Rowe JM. Hyperleukocytic leukemias: rheological, clinical, and therapeutic considerations. Blood 1982; 60: 279-283. PMID: 7046844
6. Stucki A, Rivier AS, Gikic M, Monai N, Schapira M, Spertini O. Endothelial cell activation by myeloblasts: molecular mechanisms of leukostasis and leukemic cell dissemination. Blood 2001; 97: 2121-2129. doi: 10.1182/blood.v97.7.2121.
7. McKee LC, Jr., Collins RD. Intravascular leukocyte thrombi and aggregates as a cause of morbidity and mortality in leukemia. Medicine (Baltimore) 1974; 53: 463-478. doi: 10.1097/00005792-197411000-00006.
8. Howard SC, Jones DP, Pui CH. The tumor lysis syndrome. N Engl J Med 2011; 364: 1844-1854. doi: 10.1056/NEJMra0904569.
9. Dutcher JP, Schiffer CA, Wiernik PH. Hyperleukocytosis in adult acute nonlymphocytic leukemia: impact on remission rate and duration, and survival. J Clin Oncol 1987; 5: 1364-1372. doi: 10.1200/JCO.1987.5.9.1364.

10. Bug G, Anargyrou K, Tonn T, Bialleck H, Seifried E, Hoelzer D, et al. Impact of leukapheresis on early death rate in adult acute myeloid leukemia presenting with hyperleukocytosis. Transfusion 2007; 47: 1843-1850. doi: 10.1111/j.1537-2995.2007.01406.x.
11. Porcu P, Farag S, Marcucci G, Cataland SR, Kennedy MS, Bissell M. Leukocytoreduction for acute leukemia. Ther Apher 2002; 6: 15-23. doi: 10.1046/j.1526-0968.2002.00402.x.
12. Creutzig U, Rossig C, Dworzak M, Stary J, von Stackelberg A, Wossmann W, et al. Exchange Transfusion and Leukapheresis in Pediatric Patients with AML With High Risk of Early Death by Bleeding and Leukostasis. Pediatr Blood Cancer 2016; 63: 640-645. doi: 10.1002/pbc.25855.
13. Nan X, Qin Q, Gentille C, Ensor J, Leveque C, Pingali SR, et al. Leukapheresis reduces 4-week mortality in acute myeloid leukemia patients with hyperleukocytosis - a retrospective study from a tertiary center. Leuk Lymphoma 2017; 58: 1-11. doi: 10.1080/10428194.2016.1277386.
14. Gocer M, Kurtoglu E. Effect of prophylactic leukapheresis on early mortality and overall survival in acute leukemia patients with hyperleukocytosis. Ther Apher Dial 2021; 25: 697-703. doi: 10.1111/1744-9987.13645.
15. Padmanabhan A, Connelly-Smith L, Aqui N, Balogun RA, Klingel R, Meyer E, et al. Guidelines on the Use of Therapeutic Apheresis in Clinical Practice - Evidence-Based Approach from the Writing Committee of the American Society for Apheresis: The Eighth Special Issue. J Clin Apher 2019; 34: 171-354. doi: 10.1002/jca.21705.
16. Sigurbjornsson FT, Bjarnason I. Leukocytapheresis for the treatment of IBD. Nat Clin Pract Gastroenterol Hepatol 2008; 5: 509-516. doi: 10.1038/ncpgasthep1209.
17. Hanai H, Takeda Y, Eberhardson M, Gruber R, Saniabadi AR, Winqvist O, et al. The mode of actions of the Adacolumn therapeutic leucocytapheresis in patients with inflammatory bowel disease: a concise review. Clin Exp Immunol 2011; 163: 50-58. doi: 10.1111/j.1365-2249.2010.04279.x.
18. Saniabadi AR, Tanaka T, Yamamoto T, Kruis W, Sacco R. Granulomonocytapheresis as a cell-dependent treatment option for patients with inflammatory bowel disease: Concepts and clinical features for better therapeutic outcomes. J Clin Apher 2019; 34: 51-60. doi: 10.1002/jca.21670.
19. Takakura M, Shimizu M, Mizuta M, Inoue N, Tasaki Y, Ohta K, et al. Successful treatment of rituximab- and steroid-resistant nephrotic syndrome with leukocytapheresis. J Clin Apher 2018; 33: 409-411. doi: 10.1002/jca.21613.
20. Coquaz-Garoudet M, Ploin D, Pouyau R, Hoffmann Y, Baleine JF, Boeuf B, et al. Malignant pertussis in infants: factors associated with mortality in a multicenter cohort study. Ann Intensive Care 2021; 11: 70. doi: 10.1186/s13613-021-00856-y.
21. Domico M, Ridout D, MacLaren G, Barbaro R, Annich G, Schlapbach LJ, et al. Extracorporeal Membrane Oxygenation for Pertussis: Predictors of Outcome Including Pulmonary Hypertension and Leukodepletion. Pediatr Crit Care Med 2018; 19: 254-261. doi: 10.1097/PCC.0000000000001454.
22. Miyazono A, Abe J, Ogura M, Sato M, Fujimaru T, Kamei K, et al. Successful remission induced by plasma exchange combined with leukocytapheresis against refractory systemic juvenile idiopathic arthritis. Eur J Pediatr 2014; 173: 1557-1560. doi: 10.1007/s00431-013-2093-5.
23. Diaz MA, Garcia-Sanchez F, Lillo R, Vicent MG, Vicario JL, Madero L. Large-volume leukapheresis in pediatric patients: pre-apheresis peripheral blood CD34+ cell count predicts progenitor cell yield. Haematologica 1999; 84: 32-35. PMID: 10091391
24. Cecyn KZ, Seber A, Ginani VC, Goncalves AV, Caram EM, Oguro T, et al. Large-volume leukapheresis for peripheral blood progenitor cell collection in low body weight pediatric patients: a single center experience. Transfus Apher Sci 2005; 32: 269-274. doi: 10.1016/j.transci.2004.07.015.
25. Karow A, Wilhelm A, Ammann RA, Baerlocher GM, Pabst T, Mansouri Taleghani B, et al. Peripheral blood progenitor cell collection in pediatric patients optimized by high pre-apheresis count of circulating CD34+ cells and high blood flow. Bone Marrow Transplant 2019; 54: 885-893. doi: 10.1038/s41409-018-0353-8.
26. Ribeil JA, Hacein-Bey-Abina S, Payen E, Magnani A, Semeraro M, Magrin E, et al. Gene Therapy in a Patient with Sickle Cell Disease. N Engl J Med 2017; 376: 848-855. doi: 10.1056/NEJMoa1609677.
27. Thompson AA, Walters MC, Kwiatkowski J, Rasko JEJ, Ribeil JA, Hongeng S, et al. Gene Therapy in Patients with Transfusion-Dependent beta-Thalassemia. N Engl J Med 2018; 378: 1479-1493. doi: 10.1056/NEJMoa1705342.
28. Nair SK, Driscoll T, Boczkowski D, Schmittling R, Reynolds R, Johnson LA, et al. Ex vivo generation of dendritic cells from cryopreserved, post-induction chemotherapy, mobilized leukapheresis from pediatric patients with medulloblastoma. J Neurooncol 2015; 125: 65-74. doi: 10.1007/s11060-015-1890-2.
29. Maude SL, Laetsch TW, Buechner J, Rives S, Boyer M, Bittencourt H, et al. Tisagenlecleucel in Children and Young Adults with B-Cell Lymphoblastic Leukemia. N Engl J Med 2018; 378: 439-448. doi: 10.1056/NEJMoa1709866.
30. Ceppi F, Rivers J, Annesley C, Pinto N, Park JR, Lindgren C, et al. Lymphocyte apheresis for chimeric antigen receptor T-cell manufacturing in children and young adults with leukemia and neuroblastoma. Transfusion 2018; 58: 1414-1420. doi: 10.1111/trf.14569.
31. Cerwenka A, Lanier LL. Natural killers join the fight against cancer. Science 2018; 359: 1460-1461. doi: 10.1126/science.aat2184.
32. Nikolajeva O, Mijovic A, Hess D, Tatam E, Amrolia P, Chiesa R, et al. Single-donor granulocyte transfusions for improving the outcome of high-risk pediatric patients with known bacterial and fungal infections undergoing stem cell transplantation: a 10-year single-center experience. Bone Marrow Transplant 2015; 50: 846-849. doi: 10.1038/bmt.2015.53.
33. Price TH, Boeckh M, Harrison RW, McCullough J, Ness PM, Strauss RG, et al. Efficacy of transfusion with granulocytes from G-CSF/dexamethasone-treated donors in neutropenic patients with infection. Blood 2015; 126: 2153-2161. doi: 10.1182/blood-2015-05-645986.
34. Strauss RG. Safety of donating multiple products in a single apheresis collection: are we expecting too much? J Clin Apher 2003; 18: 135-140. doi: 10.1002/jca.10069.
35. Stenzinger M, Bonig H. Risks of leukapheresis and how to manage them-A non-systematic review. Transfus Apher Sci 2018; 57: 628-634. doi: 10.1016/j.transci.2018.09.008.
36. Runco DV, Josephson CD, Raikar SS, Goldsmith KC, Lew G, Pauly M, et al. Hyperleukocytosis in infant acute leukemia: a role for manual exchange transfusion for leukoreduction. Transfusion 2018; 58: 1149-1156. doi: 10.1111/trf.14512.
37. Pathiraja V, Matar AJ, Gusha A, Huang CA, Duran-Struuck R. Leukapheresis protocol for nonhuman primates weighing less than 10 kg. J Am Assoc Lab Anim Sci 2013; 52: 70-77. PMID: 23562036
38. Michon B, Moghrabi A, Winikoff R, Barrette S, Bernstein ML, Champagne J, et al. Complications of apheresis in children. Transfusion 2007; 47: 1837-1842. doi: 10.1111/j.1537-2995.2007.01405.x.
39. McLeod BC, Sniecinski I, Ciavarella D, Owen H, Price TH, Randels MJ, et al. Frequency of immediate adverse effects associated with therapeutic apheresis. Transfusion 1999; 39: 282-288. doi: 10.1046/j.1537-2995.1999.39399219285.x.
40. Woloskie S, Armelagos H, Meade JM, Haas D. Leukodepletion for acute lymphocytic leukemia in a three-week-old infant. J Clin Apher 2001; 16: 31-32. doi: 10.1002/jca.1006.
41. Rudolph AM. Rudolph's Pediatrics: McGraw-Hill, Medical Pub. Division, 2003.
42. Sisson TR, Whalen LE, Telek A. The blood volume of infants. II. The premature infant during the first year of life. J Pediatr 1959; 55: 430-446. doi: 10.1016/s0022-3476(59)80281-x.
43. Zeng F, Huang H, Fu D, Huang Q, Fan L, Wei S. Leukapheresis in 15 patients weighing 20kg or less: A single centre experience. Transfus Apher Sci 2017; 56: 889-893. doi: 10.1016/j.transci.2017.11.001.

© SIMTI PROOF

44. Thapa N, Pham R, Cole C, Meinershagen M, Bowman PW, Ray A. Therapeutic leukocytapheresis in infants and children with leukemia and hyperleukocytosis: A single institution experience. J Clin Apher 2018; 33: 316-323. doi: 10.1002/jca.21610.

45. Kim H, Lee JH, Choi SJ, Lee JH, Seol M, Lee YS, et al. Risk score model for fatal intracranial hemorrhage in acute leukemia. Leukemia 2006; 20: 770-776. doi: 10.1038/sj.leu.2404148.

46. Bojanic I, Mazic S, Rajic L, Jakovljevic G, Stepan J, Cepulic BG. Large volume leukapheresis is efficient and safe even in small children up to 15 kg body weight. Blood Transfus 2017; 15: 85-92. doi: 10.2450/2016.0151-15.

47. Doberschuetz N, Soerensen J, Bonig H, Willasch A, Rettinger E, Pfirrmann V, et al. Mobilized peripheral blood stem cell apheresis via Hickman catheter in pediatric patients. Transfusion 2019; 59: 1061-1068. doi: 10.1111/trf.15113.

48. Jarisch A, Rettinger E, Sorensen J, Klingebiel T, Schafer R, Seifried E, et al. Unstimulated apheresis for chimeric antigen receptor manufacturing in pediatric/adolescent acute lymphoblastic leukemia patients. J Clin Apher 2020; 35: 398-405. doi: 10.1002/jca.21812.

49. Elavia N, Panch SR, McManus A, Bikkani T, Szymanski J, Highfill SL, et al. Effects of starting cellular material composition on chimeric antigen receptor T-cell expansion and characteristics. Transfusion 2019; 59: 1755-1764. doi: 10.1111/trf.15287.

50. Sethu P, Sin A, Toner M. Microfluidic diffusive filter for apheresis (leukapheresis). Lab Chip 2006; 6: 83-89. doi: 10.1039/b512049g.

51. Wu Z, Chen Y, Wang M, Chung AJ. Continuous inertial microparticle and blood cell separation in straight channels with local microstructures. Lab Chip 2016; 16: 532-542. doi: 10.1039/c5lc01435b.

52. Tan JKS, Park SY, Leo HL, Kim S. Continuous Separation of White Blood Cells From Whole Blood Using Viscoelastic Effects. IEEE Trans Biomed Circuits Syst 2017; 11: 1431-1437. doi: 10.1109/TBCAS.2017.2748232.

53. Alvankarian J, Bahadorimehr A, Yeop Majlis B. A pillar-based microfilter for isolation of white blood cells on elastomeric substrate. Biomicrofluidics 2013; 7: 14102. doi: 10.1063/1.4774068.

54. Kuan DH, Wu CC, Su WY, Huang NT. A Microfluidic Device for Simultaneous Extraction of Plasma, Red Blood Cells, and On-Chip White Blood Cell Trapping. Sci Rep 2018; 8: 15345. doi: 10.1038/s41598-018-33738-8.

55. Cheng Y, Ye X, Ma Z, Xie S, Wang W. High-throughput and clogging-free microfluidic filtration platform for on-chip cell separation from undiluted whole blood. Biomicrofluidics 2016; 10: 014118. doi: 10.1063/1.4941985.

56. Prabhakar A, Kumar YVBV, Tripathi S, Agrawal A. A novel, compact and efficient microchannel arrangement with multiple hydrodynamic effects for blood plasma separation. Microfluid Nanofluid 2014; 18: 995-1006. doi: 10.1007/s10404-014-1488-6.

57. Warkiani ME, Wu L, Tay AK, Han J. Large-Volume Microfluidic Cell Sorting for Biomedical Applications. Annu Rev Biomed Eng 2015; 17: 1-34. doi: 10.1146/annurev-bioeng-071114-040818.

58. Li X, Chen W, Liu G, Lu W, Fu J. Continuous-flow microfluidic blood cell sorting for unprocessed whole blood using surface-micromachined microfiltration membranes. Lab Chip 2014; 14: 2565-2575. doi: 10.1039/c4lc00350k.

59. Guo Q, Duffy SP, Matthews K, Islamzada E, Ma H. Deformability based Cell Sorting using Microfluidic Ratchets Enabling Phenotypic Separation of Leukocytes Directly from Whole Blood. Sci Rep 2017; 7: 6627. doi: 10.1038/s41598-017-06865-x.

60. Shevkoplyas SS, Yoshida T, Munn LL, Bitensky MW. Biomimetic autoseparation of leukocytes from whole blood in a microfluidic device. Anal Chem 2005; 77: 933-937. doi: 10.1021/ac049037i.

61. Forouzan O, Yang X, Sosa JM, Burns JM, Shevkoplyas SS. Spontaneous oscillations of capillary blood flow in artificial microvascular networks. Microvasc Res 2012; 84: 123-132. doi: 10.1016/j.mvr.2012.06.006.

62. Marcogliese AN YD. Resources for the Hematologist. In: Ronald Hoffman EB, Helen Heslop, Jeffrey Weitz, ed. Hematology: Basic Principles and Practice: Elsevier, 2018.

63. Simmons A, Leaverton P, Elbert G. Normal laboratory values for differential white cell counts established by manual and automated cytochemical methods (Hemalog D-TM). J Clin Pathol 1974; 27: 55-58. doi: 10.1136/jcp.27.1.55.

64. Liu C, Hu GQ. High-Throughput Particle Manipulation Based on Hydrodynamic Effects in Microchannels. Micromachines 2017; 8: 73. doi: 10.3390/mi8030073.

65. Bhagat AAS, Kuntaegowdanahalli SS, Papautsky I. Enhanced particle filtration in straight microchannels using shear-modulated inertial migration. Phys Fluids 2008; 20: 101702. doi: 10.1063/1.2998844.

66. Ying Y, Lin Y. Inertial Focusing and Separation of Particles in Similar Curved Channels. Sci Rep 2019; 9: 16575. doi: 10.1038/s41598-019-52983-z.

67. Martel JM, Toner M. Inertial focusing in microfluidics. Annu Rev Biomed Eng 2014; 16: 371-396. doi: 10.1146/annurev-bioeng-121813-120704.

68. Di Carlo D. Inertial microfluidics. Lab Chip 2009; 9: 3038-3046. doi: 10.1039/b912547g.

69. Kuntaegowdanahalli SS, Bhagat AA, Kumar G, Papautsky I. Inertial microfluidics for continuous particle separation in spiral microchannels. Lab Chip 2009; 9: 2973-2980. doi: 10.1039/b908271a.

70. Wu L, Guan G, Hou HW, Bhagat AA, Han J. Separation of leukocytes from blood using spiral channel with trapezoid cross-section. Anal Chem 2012; 84: 9324-9331. doi: 10.1021/ac302085y.

71. Nivedita N, Papautsky I. Continuous separation of blood cells in spiral microfluidic devices. Biomicrofluidics 2013; 7: 54101. doi: 10.1063/1.4819275.

72. Zhang J, Yuan D, Sluyter R, Yan S, Zhao Q, Xia H, et al. High-Throughput Separation of White Blood Cells From Whole Blood Using Inertial Microfluidics. IEEE Trans Biomed Circuits Syst 2017; 11: 1422-1430. doi: 10.1109/TBCAS.2017.2735440.

73. Zhou J, Tu C, Liang Y, Huang B, Fang Y, Liang X, et al. Isolation of cells from whole blood using shear-induced diffusion. Sci Rep 2018; 8: 9411. doi: 10.1038/s41598-018-27779-2.

74. Zhou J, Papautsky I. Size-dependent enrichment of leukocytes from undiluted whole blood using shear-induced diffusion. Lab Chip 2019; 19: 3416-3426. doi: 10.1039/c9lc00786e.

75. Jeon H, Jundi B, Choi K, Ryu H, Levy BD, Lim G, et al. Fully-automated and field-deployable blood leukocyte separation platform using multi-dimensional double spiral (MDDS) inertial microfluidics. Lab Chip 2020; 20: 3612-3624. doi: 10.1039/d0lc00675k.

76. Huang LR, Cox EC, Austin RH, Sturm JC. Continuous particle separation through deterministic lateral displacement. Science 2004; 304: 987-990. doi: 10.1126/science.1094567.

77. Davis JA, Inglis DW, Morton KJ, Lawrence DA, Huang LR, Chou SY, et al. Deterministic hydrodynamics: taking blood apart. Proc Natl Acad Sci U S A 2006; 103: 14779-14784. doi: 10.1073/pnas.0605967103.

78. McGrath J, Jimenez M, Bridle H. Deterministic lateral displacement for particle separation: a review. Lab Chip 2014; 14: 4139-4158. doi: 10.1039/c4lc00939h.

79. Salafi T, Zhang Y, Zhang Y. A Review on Deterministic Lateral Displacement for Particle Separation and Detection. Nanomicro Lett 2019; 11: 77. doi: 10.1007/s40820-019-0308-7.

80. Civin CI, Ward T, Skelley AM, Gandhi K, Peilun Lee Z, Dosier CR, et al. Automated leukocyte processing by microfluidic deterministic lateral displacement. Cytometry A 2016; 89: 1073-1083. doi: 10.1002/cyto.a.23019.

81. Mutlu BR, Smith KC, Edd JF, Nadar P, Dlamini M, Kapur R, et al. Non-equilibrium Inertial Separation Array for High-throughput, Large-volume Blood Fractionation. Sci Rep 2017; 7: 9915. doi: 10.1038/s41598-017-10295-0.

82. Yamada M, Seko W, Yanai T, Ninomiya K, Seki M. Slanted, asymmetric microfluidic lattices as size-selective sieves for continuous particle/cell sorting. Lab Chip 2017; 17: 304-314. doi: 10.1039/c6lc01237j.

83. Campos-Gonzalez R, Skelley AM, Gandhi K, Inglis DW, Sturm JC, Civin CI, et al. Deterministic Lateral Displacement: The Next-Generation CAR T-Cell Processing? SLAS Technol 2018; 23: 338-351. doi: 10.1177/2472630317751214.

© SIMTIPRO Srl

84. Lipowsky HH. Microvascular rheology and hemodynamics. Microcirculation 2005; 12: 5-15. doi: 10.1080/10739680590894966.

85. Schmid-Schonbein GW, Usami S, Skalak R, Chien S. The interaction of leukocytes and erythrocytes in capillary and postcapillary vessels. Microvasc Res 1980; 19: 45-70. doi: 10.1016/0026-2862(80)90083-7.

86. Forouzan O, Burns JM, Robichaux JL, Murfee WL, Shevkoplyas SS. Passive recruitment of circulating leukocytes into capillary sprouts from existing capillaries in a microfluidic system. Lab Chip 2011; 11: 1924-1932. doi: 10.1039/c0lc00547a.

87. Yang X, Forouzan O, Burns JM, Shevkoplyas SS. Traffic of leukocytes in microfluidic channels with rectangular and rounded cross-sections. Lab Chip 2011; 11: 3231-3240. doi: 10.1039/c1lc20293f.

88. Jain A, Munn LL. Determinants of leukocyte margination in rectangular microchannels. PLoS One 2009; 4: e7104. doi: 10.1371/journal.pone.0007104.

89. Jain A, Munn LL. Biomimetic postcapillary expansions for enhancing rare blood cell separation on a microfluidic chip. Lab Chip 2011; 11: 2941-2947. doi: 10.1039/c1lc20401g.

90. Kim B, Choi YJ, Seo H, Shin EC, Choi S. Deterministic Migration-Based Separation of White Blood Cells. Small 2016; 12: 5159-5168. doi: 10.1002/smll.201601652.

91. Choi S, Song S, Choi C, Park JK. Hydrophoretic sorting of micrometer and submicrometer particles using anisotropic microfluidic obstacles. Anal Chem 2009; 81: 50-55. doi: 10.1021/ac801720x.

92. Inglis DW, Herman N. A scalable approach for high throughput branch flow filtration. Lab Chip 2013; 13: 1724-1731. doi: 10.1039/c3lc50192b.

93. Yang S, Undar A, Zahn JD. A microfluidic device for continuous, real time blood plasma separation. Lab Chip 2006; 6: 871-880. doi: 10.1039/b516401j.

94. Gifford SC, Spillane AM, Vignes SM, Shevkoplyas SS. Controlled incremental filtration: a simplified approach to design and fabrication of high-throughput microfluidic devices for selective enrichment of particles. Lab Chip 2014; 14: 4496-4505. doi: 10.1039/c4lc00785a.

95. Xia H, Strachan BC, Gifford SC, Shevkoplyas SS. A high-throughput microfluidic approach for 1000-fold leukocyte reduction of platelet-rich plasma. Sci Rep 2016; 6: 35943. doi: 10.1038/srep35943.

96. Strachan BC, Xia H, Voros E, Gifford SC, Shevkoplyas SS. Improved expansion of T cells in culture when isolated with an equipment-free, high-throughput, flow-through microfluidic module versus traditional density gradient centrifugation. Cytotherapy 2019; 21: 234-245. doi: 10.1016/j.jcyt.2018.12.004.

97. Lezzar DL, Lam FW, Huerta R, Mukhamedshin A, Lu M, Shevkoplyas SS. A high-throughput microfluidic device based on controlled incremental filtration to enable centrifugation-free, low extracorporeal volume leukapheresis. Sci Rep 2022; 12: 13798. doi: 10.1038/s41598-022-16748-5.

98. Goldstein SL. Therapeutic apheresis in children: special considerations. Semin Dial 2012; 25: 165-170. doi: 10.1111/j.1525-139X.2011.01028.x.

99. Kornbau C, Lee KC, Hughes GD, Firstenberg MS. Central line complications. Int J Crit Illn Inj Sci 2015; 5: 170-178. doi: 10.4103/2229-5151.164940.

100. Oberoi S, Lehrnbecher T, Phillips B, Hitzler J, Ethier MC, Beyene J, et al. Leukapheresis and low-dose chemotherapy do not reduce early mortality in acute myeloid leukemia hyperleukocytosis: a systematic review and meta-analysis. Leuk Res 2014; 38: 460-468. doi: 10.1016/j.leukres.2014.01.004.

101. Landzo E, Sofo-Hafizovic A, Cetkovic-Basic V. Initial values of donor hematocrit and efficiency of plateletpheresis. Acta Inform Med 2013; 21: 116-119. doi: 10.5455/aim.2013.21.116-119.

102. Lindholm-Perry AK, Kuehn LA, Wells JE, Rempel LA, Chitko-McKown CG, Keel BN, et al. Hematology parameters as potential indicators of feed efficiency in pigs. Transl Anim Sci 2021; 5: txab219. doi: 10.1093/tas/txab219.

© SIMTIPRO Srl